Thermoelectric properties of Mn-doped iron disilicide ceramics fabricated from radio-frequency plasma-treated fine powders

T. TOKIAI
Idemitsu Kosan Co. Ltd, 24-4, Anegasaki-kaigan, Ichihara, Chiba 299-01, Japan

T. UESUGI, M. NOSAKA, A. HIRAYAMA, K. ITO
Idemitsu Petrochemical Co. Ltd, 3-3-1, Marunouchi, Chiyoda-ku, Tokyo 100, Japan

K. KOUMOTO
Department of Applied Chemistry, School of Engineering, Nagoya University, Furo-cho, Chikusa-ku, Nagoya 464-01, Japan

Fine particles of $Fe_{0.92}Mn_{0.08}Si_{2.00}$, 200 nm in size, were produced using a high-frequency plasma. The powders were sintered at temperatures between 1323 and 1423 K in vacuum and then heat treated at 1073 K to transform them into thermoelectric semiconducting iron disilicide. The relative density of the samples was as low as 70–77%, and the microstructure was composed of several tens of micrometre grains and continuous pores. The sample sintered at 1423 K, in particular, showed a figure of merit, Z, of $2.0 \times 10^{-4}\,K^{-1}$ at 870 K which was 20% larger than those previously reported. The increase in Z was found to be attributable to the increase in Seebeck coefficient and the decrease in thermal conductivity.

1. Introduction

Sintered ceramics of $FeSi_2$ feature a high heat resistance, high oxidation resistance and large thermoelectromotive force. Therefore, they have attracted much attention as high-temperature thermoelectric materials to be used in an atmosphere of household gas and in petroleum equipment. According to the phase diagram reported by Piton and Fay [1], the $FeSi_2$ composition corresponds to a eutectic alloy consisting of ε-$FeSi_2$ and α-Fe_2Si_5, both of which show metallic conductivity between the eutectic temperature, 1485 K, and the peritectic temperature, 1259 K. Below 1259 K, the alloy turns into a single phase of β-$FeSi_2$ whose stoichiometric composition exhibits a semiconducting nature. It is known that β-$FeSi_2$ is an intrinsic semiconductor, and that with the addition of Al or Mn it will turn into a p-type semiconductor, and with the addition of Co into an n-type semiconductor [2].

As regards the preparation of the thermoelectric materials of $FeSi_2$, the optimum sintering conditions of the powder which is several micrometres in size and the following heat treatment conditions to produce the semiconducting phase are currently well known [3]. In contrast, it has just recently become possible to fabricate the thermoelectric materials of $FeSi_2$ from fine particles of submicrometre size, and this paper reports their thermoelectric properties and electrical conduction mechanism.

2. Experimental procedure

2.1. Preparation of fine particles of $FeSi_2$ [4–7]

We selected the composition of $Fe_{0.92}Mn_{0.08}Si_{2.00}$ for the experiment, since it was known as a p-type semiconductor to generate the highest figure of merit. Commercially available powder of 99.9% purity was vacuum melted in a high-frequency induction furnace, and ingots of $Fe_{0.92}Mn_{0.08}Si_{2.00}$ composition were produced. The ingots were pulverized into the powder of several tens of micrometres using a stamp mill. This powder was turned into granules 0.5 mm in diameter by adding 1 wt % of poly(vinyl alcohol) as a binder. The granules screened to 48–150 mesh were subjected to radio-frequency (r.f.) plasma treatment. Table I shows the composition of the initial powder.

The granules were fed into high-frequency (4 MHz) Ar–H_2 plasma under atmospheric pressure at a rate of $1.0\,g\,min^{-1}$ to produce fine particles. A schematic diagram of the high-frequency plasma is shown in Fig. 1. Plasma was generated inside a quartz tube 57 mm in inside diameter and 150 mm long, while Ar gas was introduced through nozzles 1, 2 and 3 with H_2 gas through nozzle 2. The end of nozzle 3 was placed in the centre of the three-turn coil, where the granules were introduced to produce the fine particles [8, 9].

0022–2461

TABLE I Composition of the starting material.

Composition	
Element	Amount (wt %)
Fe	44.90
Si	50.46
Mn	3.91
Al	0.36
Ca	0.014
Ti	0.134

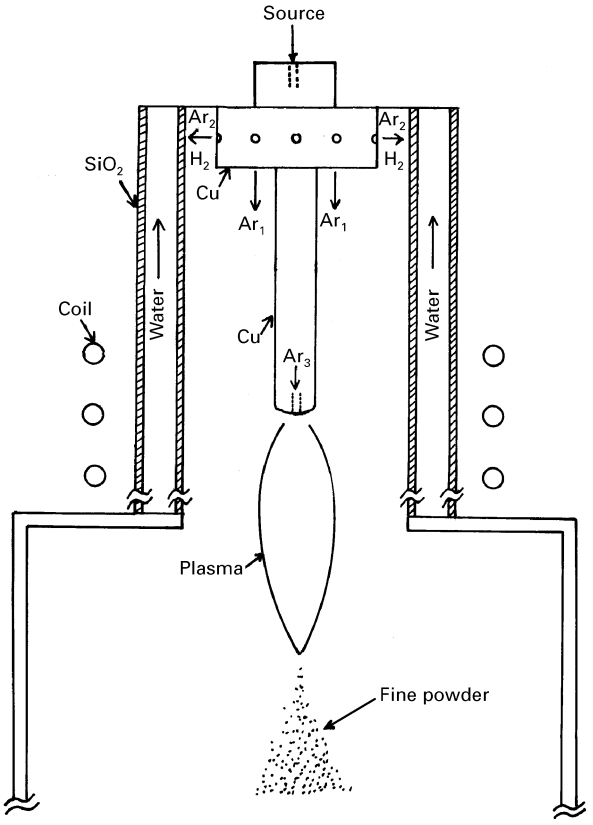

Figure 1 Schematic illustration of the r.f. plasma torch.

2.2. Moulding and sintering [10]

The fine particles were moulded under a pressure of 1.8×10^7 Pa by a spindle press into rectangular bars 2 mm × 5.4 mm × 30 mm to measure the electrical resistivity and Seebeck coefficient. Disc specimens 10 mm in diameter and 2 mm thick were also fabricated to measure thermal conductivity.

Moulded compacts were pre-heated in air from room temperature to 673 K, and the binder and the adsorbed impurities were removed completely. Then, in a vacuum of 1.33×10^{-3} Pa, they were sintered at 1323 − 1423 K for 24 h. Sintered samples were further annealed at 1073 K for 200 h in vacuum.

2.3. Measurements

The average size of the fine particles obtained was determined using a transmission electron microscope (JEOL JEM-100). The density of the sintered sample was measured by the Archimedean method. The impurity oxygen content was measured with an oxygen–nitrogen analyser (Leco Co. TC436).

The temperature dependences of resistivity and Seebeck coefficient were measured at 300–1400 K in vacuum using the direct-current four-probe method reported by Nishida and Sakata [11]. The temperature was measured with Pt–(Pt–13% Rh) thermocouples. Thermal conductivity was measured at 300–1400 K using the laser-flash method (Rigaku Co. TCM-FA851013) [12].

3. Results and discussion

3.1. Characteristics of fine powder

Fig. 2 shows a transmission electron micrograph of the fine particles (average size, 200 nm) produced under the conditions listed in Table II. Although the initial powder was composed of the particles several micrometres in size with an irregular shape, the particles produced are very fine and spherical, possibly because the powder introduced into an Ar–H_2 high-temperature plasma gas of 10 000 K evaporated once and then condensed at an ultrahigh speed in the tail part of the plasma.

The X-ray diffraction (XRD) pattern of the fine powder obtained is shown in Fig. 3. Although the initial powder consisted only of metallic α and ε phases, the fine particles contained semiconducting β phase as well as α and ε phases [1]. The oxygen content of the fine powder was found to be 0.24 wt %.

3.2. Sintering of fine powders

Green compacts of fine powders were sintered at 1323–1423 K for 24 h in vacuum (1.33×10^{-3} Pa). Fig. 4 shows the relationship between the sintering temperature and the relative density of the samples. As the sintering temperature increased, the relative density increased only up to about 77% at 1423 K. Compared with an ordinary powder, the relative density obtained is rather low. According to Kojima *et al.* [13], 77% relative density corresponds to the intermediate stage of sintering. The low sinterability of fine powders must have been due to their inhomogeneous compaction caused by the particle agglomeration in-

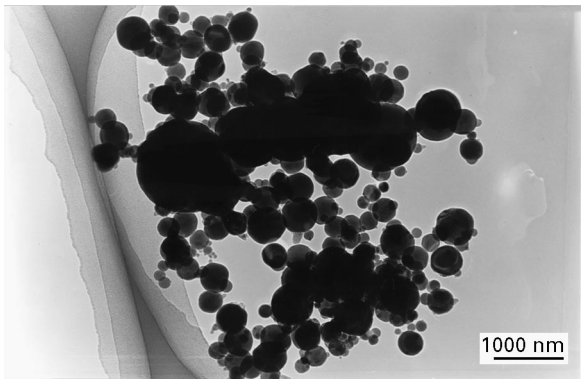

Figure 2 Transmission electron micrograph of fine particles.

TABLE II R.f. plasma conditions for the preparation of fine powders.

Power (kW)	Pressure (atm)	Ar flow rate ($l\,min^{-1}$)			H_2 flow rate nozzle 2 ($l\,min^{-1}$)
		Nozzle 1	Nozzle 2	Nozzle 3	
34.0	1.0	10	20	30	2.0

Feed, 1.0 $g\,min^{-1}$.

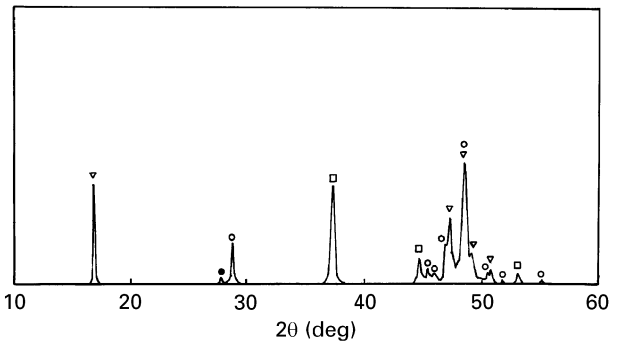

Figure 3 XRD pattern of fine particles obtained by the r.f. plasma method. (○), β-$FeSi_2$; (▽), α-Fe_2Si_5; (□), ε-FeSi; (●), Si.

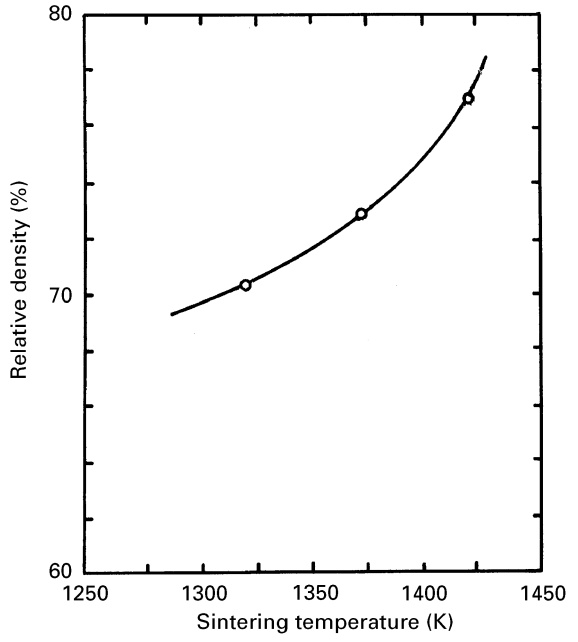

Figure 4 Correlation between relative density and sintering temperature.

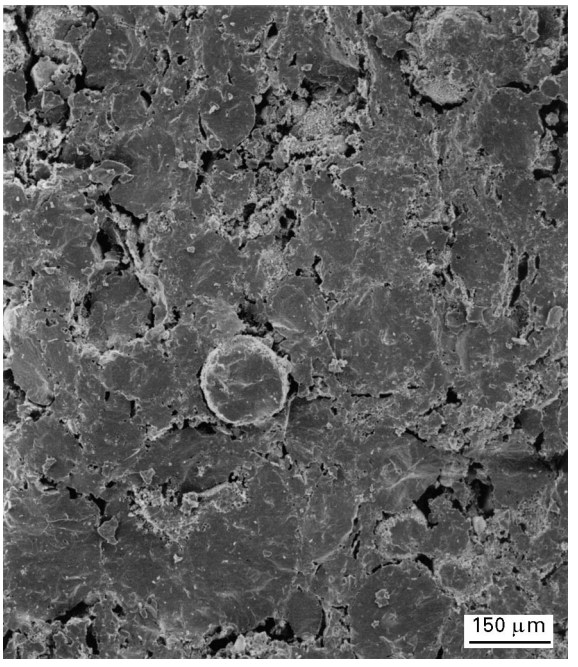

Figure 5 Scanning electron micrograph of the sintered body at 1423 K.

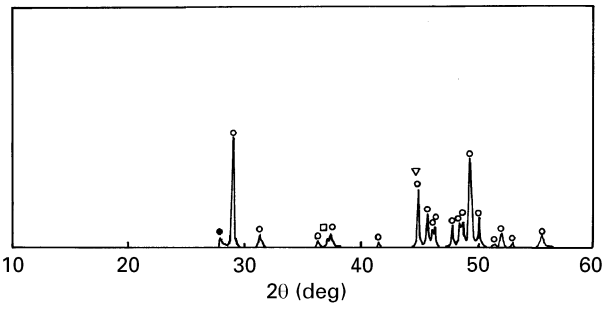

Figure 6 XRD pattern of the sintered body at 1423 K. (○), β-$FeSi_2$; (▽), α-Fe_2Si_5; (□), ε-FeSi; (●), Si.

hibiting the homogeneous densification. The impurity oxygen would also have affected the sintering process, although its role is not known well.

Figs 5 and 6 show a typical scanning electron micrograph and an XRD pattern respectively, of the sintered sample. It is evident that the crystal grains grew into spheres of several tens of micrometres in size indicating that enhanced grain growth had taken place. Continuous open pores can also be seen in the microstructure.

The XRD pattern of the pulverized powder shows that β-$FeSi_2$ is predominantly formed with small amounts of Si, and α and ε phases.

3.3. Seebeck coefficient and resistivity

Fig. 7 shows the temperature dependence of the Seebeck coefficient for the sintered compacts fabricated from the fine powder. The Seebeck coefficient decreased with increasing sintering temperature. For each sintering temperature the Seebeck coefficient increased with increasing temperature up to 400–600 K, became almost constant in the temperature range 600–800 K and then decreased above 800 K.

The Seebeck coefficient is known to decrease as the carrier concentration increases with increasing temperature by Ioffe's theory [14]. However, the observed Seebeck coefficient does not decrease until the temperature reaches 800 K, and this appears to be inconsistent

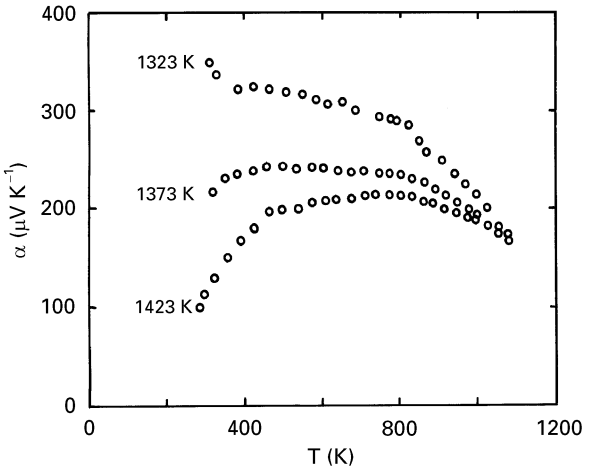

Figure 7 Temperature dependence of the Seebeck coefficient.

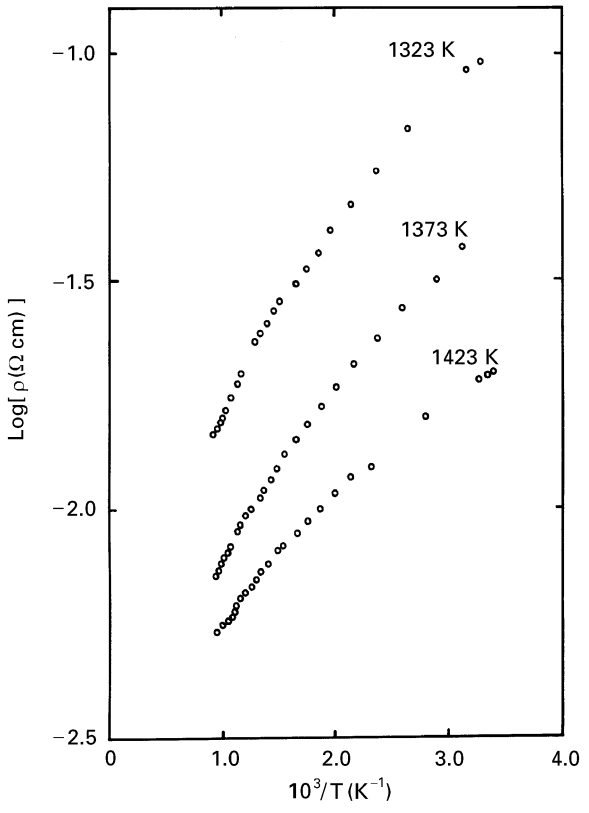

Figure 8 Temperature dependence of the resistivity.

with the theory. Such an anomalous temperature dependence of Seebeck coefficient has been observed by several workers [13, 15–17].

Fig. 8 shows that the resistivity, ρ, of iron disilicide decreases with increasing sintering temperature. The ρ versus $1/T$ relationship can be divided into two temperature regions: firstly the extrinsic region, room temperature $< T \lesssim 700$ K; secondly the intrinsic region, $T \gtrsim 700$ K. The slope of the straight line drawn through the data points corresponds to the acceptor level, E_a, in the extrinsic region and the band-gap energy, E_g, in the intrinsic region. Both E_a and E_g slightly decreased with increasing sintering temperature and were calculated to be 0.08–0.03 eV and 0.8–0.7 eV, respectively. These values agree well with

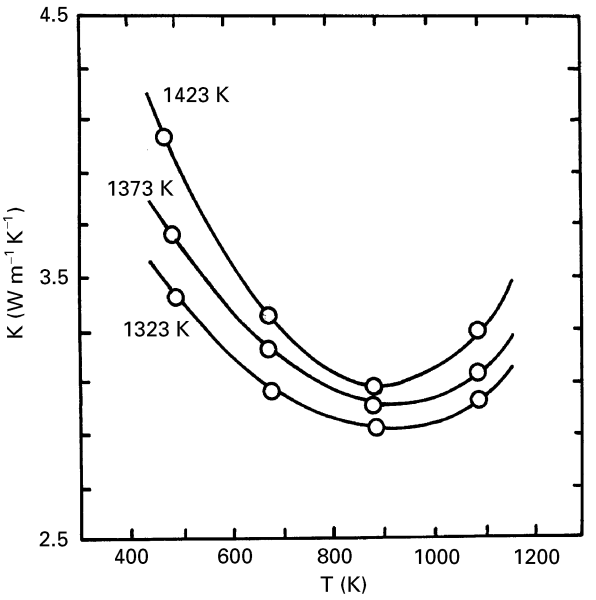

Figure 9 Temperature dependence of the thermal conductivity.

those reported in the literature [15, 18], even though the specimens employed for the measurement in the present study are relatively porous (70–77% of the theoretical density). The variation in these values with sintering temperature is thought to have been caused by porous microstructure.

3.4. Thermal conductivity and figure of merit

Fig. 9 shows the temperature dependence of the thermal conductivity, κ, of the sintered samples. The thermal conductivity of sintered samples decreased and then increased with increasing temperature, going through the minimum value at about 900 K. The minimum thermal conductivity of the sample sintered at 1323 K obtained at 900 K was 2.9 $w\,m^{-1}\,k^{-1}$. The thermal conductivity of the present porous specimens is much smaller on the whole than that reported for the dense iron disilicide added with Al [13, 15, 19, 20], Co [13, 15, 19–21] and Mn [13, 15].

A remarkable feature observed in the temperature dependence of κ is that it showed a minimum at about 900 K; a monotonic decrease in κ has been observed for dense sintered specimens [13]. The thermal conductivity, κ, in general, is roughly composed of the phonon contribution, κ_{ph}, and the carrier contribution, κ_{car}: $\kappa = \kappa_{ph} + \kappa_{car}$. Accordingly, κ was lowered possibly owing to the phonon–phonon scattering [18] and, as the temperature was elevated, the increase in κ due to the increase in carrier density as suggested by decreasing resistivity must have increased the total thermal conductivity, giving a minimum at high temperatures.

The performance of a thermoelectric material can be evaluated in terms of the figure of merit, Z, expressed as

$$Z\,(K^{-1}) = \frac{\alpha^2}{\kappa}\rho \qquad (1)$$

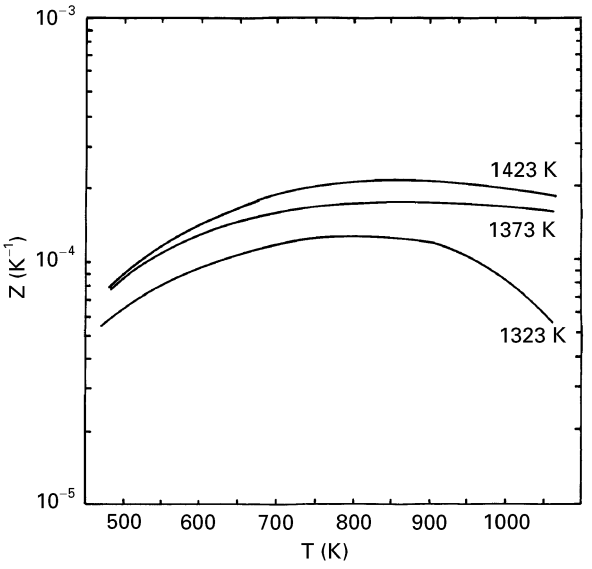

Figure 10 Correlation between the figure of merit and the temperature.

Fig. 10 shows the temperature dependence of the figure of merit of the sintered samples. The figure of merit, Z, of the sample sintered at 1423 K was represented by a curve showing the maximum value of $2.0 \times 10^{-4}\,K^{-1}$ at 870 K. This maximum is 20% larger than those of the dense samples reported by Kojima *et al.* [13] and Hesse and Bucksch [2]. Moreover, the Z obtained was larger in the whole temperature range than that of Mn-doped iron disilicide reported so far [13].

Consequently, it is clear that the thermoelectric semiconductor of Mn-doped iron disilicide fabricated from fine particles exhibits excellent performance since it has a high figure of merit because of high Seebeck coefficient in the temperature range 600–800 K and low thermal conductivity due to enhanced phonon scattering in porous microstructure.

4. Conclusion

Through our research on an $FeSi_2$ thermoelectric semiconductor produced from fine $FeSi_2$ particles added with Mn as the initial material, we have obtained the following understanding as to the sintering conditions and thermoelectric properties.

Fine particles of $Fe_{0.92}Mn_{0.08}Si_{2.00}$ of size 200 nm to submicrons, featuring a mixture of semiconductor phase and metallic phase, can be produced by treating $Fe_{0.92}Mn_{0.08}Si_{2.00}$ powder of several micrometres size with a high r.f. plasma.

The relative density of sintered material made from the initial powder of fine particles is low at about 80%. The dominant phase of the material is β phase. The observed structure contains spherically grown crystal grains of several tens of micrometres, primary recrystallization and continuous pores of several tens of micrometres. It represents a microstructure in which the grain growth has not grown normally into nearly equal sizes in the final process of sintering.

In particular, when the material was sintered at 1423 K for 24 h and heated at 1073 K for 144 h, the figure of merit, Z at 870 K reached

$$Z = 2.0 \times 10^{-4}\,K^{-1}$$

The increase in Z is attributable to the decrease in thermal conductivity due to enhanced phonon scattering in porous microstructure.

From these results, we conclude that the thermoelectric semiconductor of iron disilicide made from the initial powder of fine particles has the possibilities of a high-performance figure of merit, if the microstructure is controlled properly by the sintering and heat treatment conditions.

Acknowledgements

The authors are grateful to Mrs K. Aso and Mrs H. Taniyama for sample preparation and measurements.

References

1. J. P. PITON and M. F. FAY, *C. R. Acad. Sci. Paris, C* **266** (1968) 514.
2. J. HESSE and R. BUCKSCH, *J. Mater. Sci.* **5** (1970) 272.
3. F. D. RICHARDSON and J. H. E. JEFFES, *J. Iron Steel Inst., London* **171** (1952) 165.
4. H. U. ECKERT, *High Temp. Sci.* **6** (1974) 99.
5. B. WALDIE, *Chem. Engng, London* **92** (1972) 259.
6. B. WALDIE, *ibid* **188** (1972) 261.
7. R. MAHE, in "Les hautes temperatures leurs utilizations en physique et en chimie, Vol. I, edited by G. Chaudron and F. Trombe, (Masson, Paris 1973) p. 139.
8. R. M. SALINGER, *Ind. Engng Chem., Res. Dev.* **230** (1972) 11.
9. I. M. MACKINNON and B. G. REUBEN, *J. Electrochem. Soc.* **122** (1975) 806.
10. T. KOJOMA, T. MASUMOTO and I. NISHIDA, *J. Jpn. Inst. Metals* **48** (1984) 843.
11. I. NISHIDA and T. SAKATA, *J. Phys. Chem. Solids* **39** (1978) 499.
12. T. MITSUHASHI, F. MUTA, T. CHIBA and Y. FUJIKI, *Rigaku-Denki J.* **19** (1988) 16.
13. T. KOJIMA, N. HIROYAMA and M. SAKATA, *J. Mater. Sci. Soc. Jpn* **28** (1991) 22.
14. D. ADLER and H. BROOKS, *Phys. Rev.* **155** (1967) 826.
15. T. KOJIMA, *Phys. Status Solidi (a)* **111** (1989) 233.
16. Y. ISODA, T. OHKOSHI, I. NISHIDA and H. KAIBE, *J. Mater. Sci. Soc. Jpn.* **25** (1989) 311.
17. U. BIRKHOLZ and J. SCHELM, *Phys. Status Solidi (a)* **27** (1986) 413.
18. I. NISHIDA, *Phys. Rev. B* **7** (1973) 2710.
19. J. HESSE, *Z. Metallkde* **60** (1969) 652.
20. J. HESSE, *Z. Angew. Phys.* **28** (1969) 133.
21. R. M. WARE and D. J. McNEILL, *Proc. Instn Electr. Eng.* **111** (1964) 178.

Received 18 December 1995
and accepted 4 December 1996